Deficiency of Lipid Phosphatase SHIP Enables Long-Term Reconstitution of Hematopoietic Inductive Bone Marrow Microenvironment

Olin D. Liang,[1,2,3] Jiayun Lu,[1,2,3] César Nombela-Arrieta,[1,2,3] Jia Zhong,[1,2,3] Li Zhao,[1,2,3] Gregory Pivarnik,[1,2,3] Subhanjan Mondal,[1,2,3] Li Chai,[1,2,4] Leslie E. Silberstein,[1,2,3] and Hongbo R. Luo[1,2,3,*]

[1]Department of Pathology, Harvard Stem Cell Institute, Harvard Medical School, Boston, MA 02115, USA
[2]Dana-Farber/Harvard Cancer Center, Boston, MA 02115, USA
[3]Stem Cell Program and Department of Laboratory Medicine, Children's Hospital Boston, Boston, MA 02115, USA
[4]Brigham and Women's Hospital, Boston, MA 02115, USA
*Correspondence: hongbo.luo@childrens.harvard.edu
http://dx.doi.org/10.1016/j.devcel.2013.04.016

SUMMARY

A dysfunctional bone marrow (BM) microenvironment is thought to contribute to the development of hematologic diseases. However, functional replacement of pathologic BM microenvironment through BM transplantation has not been possible. Furthermore, the study of hematopoietic inductive BM microenvironment is hampered by the lack of a functional nonhematopoietic reconstitution system. Here, we show that a deficiency of SH2-containing inositol-5′-phosphatase-1 (SHIP) in a nonhematopoietic host microenvironment enables its functional reconstitution by wild-type donor cells. This microenvironment reconstitution normalizes hematopoiesis in peripheral blood and BM and alleviates pathology of spleen and lung in the SHIP-deficient recipients. SHIP-deficient BM contains a significantly smaller population of multipotent stromal cells with distinct properties, which may contribute to the reconstitution by wild-type cells. We further demonstrate that it is the nonhematopoietic donor cells that are responsible for the reconstitution. Thus, we have established a nonhematopoietic BM microenvironment reconstitution system to functionally study specific cell types in hematopoietic niches.

INTRODUCTION

The concept of hematopoietic stem cell (HSC) was first proven by Till and McCulloch following their pioneer studies of blood system regeneration in vivo (Till and McCulloch, 1961). A wealth of experimentation since then formed a solid foundation for stem cell research (Orkin and Zon, 2008). Nonhematopoietic cells within the bone marrow (BM) are collectively referred to as the BM microenvironment, which is essential for the maintenance and function of the HSCs (Bianco, 2011; Morrison and Spradling, 2008; Purton and Scadden, 2008; Schofield, 1978; Taichman, 2005). Nonhematopoietic cell types including mesenchymal-derived osteoblasts, endothelial cells, and subendothelial reticular cells (pericytes) have been detected in the BM microenvironment and have demonstrated concerted roles in regulating hematopoiesis (Calvi et al., 2003; Ding et al., 2012; Kiel et al., 2005; Omatsu et al., 2010; Sacchetti et al., 2007; Sugiyama et al., 2006; Zhang et al., 2003). Currently evolving concepts hypothesize that quiescent, long-term repopulating cells are in contact with the osteoblasts whereas more committed and proliferating hematopoietic stem and progenitor cells are in contact with the vasculature. However, in vivo imaging also suggested that the dichotomy between the endosteal and vascular niche is anatomically impossible (Lo Celso et al., 2009; Xie et al., 2009). Thus, the nature of the BM microenvironment and the relative contribution of each niche component to hematopoiesis remain elusive.

The study of HSCs has flourished after the establishment of a functional reconstitution assay in which the donor HSCs home to the marrow niches, engraft, proliferate, and eventually reconstitute the whole hematologic and immunologic repertoire of the lethally or sublethally irradiated recipient mice (Spangrude et al., 1988). In comparison, the study of the BM microenvironment is lagging far behind, partially due to the lack of a model system to functionally study individual cell types involved in the BM microenvironment through nonhematopoietic reconstitution. A search for strategies to reconstitute the BM microenvironment is warranted.

A dysfunctional BM microenvironment is now believed to contribute to the development of hematologic diseases such as myeloproliferative syndrome, myelodysplasia, leukemia, and multiple myeloma (Lane et al., 2009). In hematologic malignancies, there are dynamic interactions between leukemic cells and cells of the BM microenvironment. Recent studies indicate that leukemogenic events in the hematopoietic system may create a tumor microenvironment (Colmone et al., 2008) or transform the niche into a milieu with dominant signals promoting and sustaining abnormal cell growth (Jones and Wagers, 2008; Li and Neaves, 2006). On the other hand, experiments in which selective gene targeting within BM microenvironment leading to deletion of the retinoic acid receptor γ (Walkley et al., 2007a), retinoblastoma (Walkley et al., 2007b), or Dicer1 specifically in osteoprogenitors (Raaijmakers et al., 2010) have provided critical evidence for genetic changes in the microenvironment
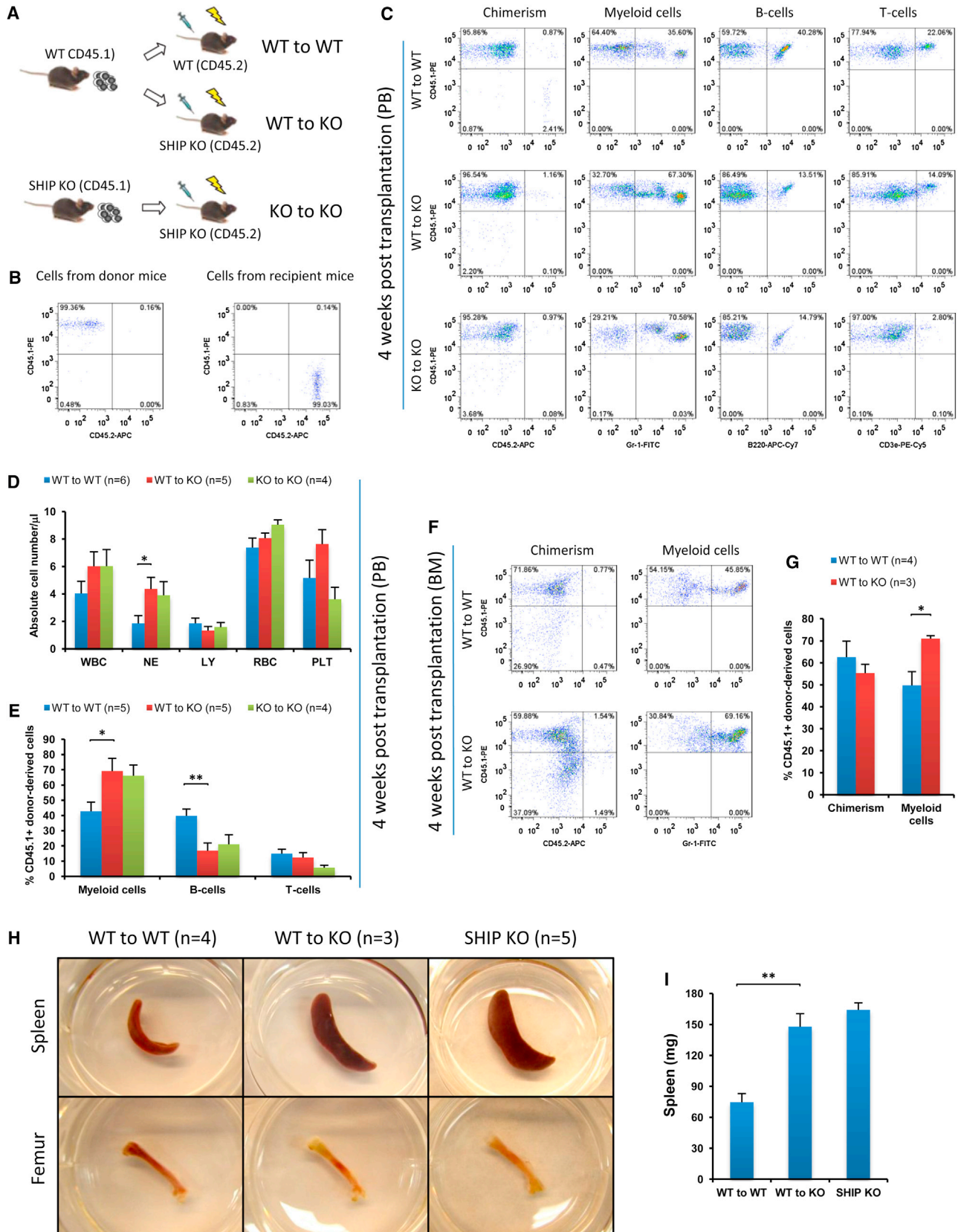
(legend on next page)

contributing to or required for leukemogenesis. Furthermore, donor-cell-derived hematopoietic disease is a well-recognized occurrence in allogeneic BM transplant recipients (Flynn and Kaufman, 2007), which provides clinical evidence implicating the BM microenvironment in leukemia development. In addition, multiple myeloma is an incurable blood disease characterized by clonal proliferation of malignant plasma cells, where the BM microenvironment has a pivotal role in tumor pathogenesis (Raab et al., 2009). A complex interplay is involved in these hematologic diseases and provides a rationale for targeting the BM microenvironment. However, functional reconstitution of a pathologic BM microenvironment through BM transplantation has not been possible. In standard irradiation and chemical ablation, the BM stroma remained functionally intact, where damaged sinusoidal endothelial cells could be replaced by host endothelial cells (Bierkens et al., 1991; Li et al., 2008). Thus, novel strategies to replace a diseased BM microenvironment are needed.

SH2-containing inositol-5′-phosphatase-1 (SHIP) hydrolyzes the phosphatidylinositol-3-kinase (PI3K) product phosphatidylinositol-3,4,5-triphosphate [PI(3,4,5)P3] to PI(3,4)P2. SHIP blunts PI3K-initiated signaling and prevents membrane recruitment and activation of pleckstrin homology domain-containing kinases (e.g., AKT and PDK) that serve as effectors of PI3K signaling (Rohrschneider et al., 2000). Within the SHIP-deficient mice a chronic progressive hyperplasia of myeloid cells was observed, perhaps at the expense of B-cell production. SHIP knockout (KO) myeloid progenitors had enhanced responsiveness to cytokines and were less susceptible to apoptotic stimuli in vitro. Increased proliferation and decreased apoptosis may also contribute to the expanded HSC compartment in SHIP KO mice, though these HSCs have compromised homing and repopulating ability (Desponts et al., 2006; Helgason et al., 1998, 2003; Liu et al., 1999). SHIP was initially thought to be restricted to hematopoietic cells, but it is now apparent that most cells of the BM and blood express SHIP. Hazen et al. demonstrated SHIP expression and participation in the function of nonhematopoietic cells of the BM, and SHIP KO mice had elevated levels of a number of hematopoietic cytokines in the serum (Hazen et al., 2009). In current study, we discovered that deficiency of SHIP in a nonhematopoietic host microenvironment could efficiently enable its functional reconstitution by wild-type (WT) nonhematopoietic donor cells. Thus, we have established a model reconstitution system to functionally study specific cell types in the hematopoietic niches.

RESULTS

A SHIP-Deficient Niche Leads to Impaired Hematopoiesis

Consistent with the reported data, we observed that SHIP KO mice had significantly higher myeloid population and lower B-cell population in both peripheral blood (PB) and the BM compared to WT mice (data not shown). To provide direct evidence that SHIP disruption in the HSC niche is responsible for the observed hematopoiesis defect, we performed reverse transplantation experiments where whole BM cells from CD45.1[+] WT mice were intravenously transplanted into lethally irradiated CD45.2[+] WT or SHIP KO mice. As a control, whole BM cells from CD45.1[+] SHIP KO mice were transplanted into lethally irradiated CD45.2[+] SHIP KO mice (Figures 1A and 1B). Four weeks after transplantation, all three experimental groups (WT-to-WT, WT-to-KO, and KO-to-KO) achieved equally high chimerism in PB (CD45.1-PE[+] and CD45.2-APC[−] populations; Figure 1C). Both complete blood cell count and lineage analysis indicated that WT-to-KO and KO-to-KO recipients exhibited a SHIP KO hematopoietic phenotype, where CD45.1[+] donor-derived hematopoietic cells produced a significantly higher myeloid population and a significantly lower B-cell population in PB compared to WT-to-WT recipients (Figures 1D and 1E). Similar to what was observed in PB, despite a comparable donor-cell chimerism in the BM (CD45.1-PE[+] and CD45.2-APC[−] populations), the donor-derived myeloid cell population in WT-to-KO recipients was significantly higher than that of the WT-to-WT recipients (Figures 1F and 1G). Earlier studies (Helgason et al., 1998; Liu et al., 1999) as well as our own observation indicated that SHIP KO mice suffer from profound splenomegaly and have fewer red blood cells in the BM than WT mice. Large spleen and pale femurs were phenotypical characteristics of SHIP KO mice. The spleen size and femoral appearance between WT-to-WT and WT-to-KO recipients remained readily distinguishable, with the latter nearly identical to those of the SHIP KO mice (Figures 1H and 1I). In addition, we transplanted whole BM cells from CD45.2[+] SHIP KO mice into lethally irradiated CD45.1[+] WT recipients. The results at 4 weeks after transplantation indicated that SHIP KO cells had a diminished ability to form chimerism in WT recipients. However, the levels of SHIP KO donor-derived myeloid cells and B cells were comparable to those of the WT-to-WT recipient mice (Figure 2). Taken together, these results suggested that SHIP deficiency in the BM microenvironment was responsible for the defective hematopoietic phenotype observed in the SHIP KO mice.

Figure 1. SHIP Deficiency in the BM Microenvironment Determined Defective Hematopoiesis at 4 Weeks Posttransplantation
(A) BM cells of CD45.1 WT mice were transplanted into lethally irradiated CD45.2 WT mice or littermate SHIP KO mice. As a control, BM cells of CD45.1 SHIP KO mice were also transplanted into lethally irradiated CD45.2 SHIP KO mice.
(B) Examples of genotyping by FACS analysis of CD45.1[+] SHIP KO mice (left, cells from donor mice) and CD45.2[+] SHIP KO mice (right, cells from recipient mice).
(C) Representative FACS profiles of hematopoietic cell lineage analysis in PB of transplant recipients.
(D and E) Absolute blood cell number (D) and donor-derived blood cell composition (E) in PB of transplant recipients.
(F and G) Transplanted WT BM cells acquired a SHIP KO hematopoietic phenotype in the BM of SHIP KO recipient mice 4 weeks after reverse transplantation. Shown are donor chimerism (similar for both WT-to-WT and WT-to-KO) and donor-derived myeloid cell populations (higher in WT-to-KO than in WT-to-WT).
(H and I) Transplantation of WT BM cells to the SHIP KO mice could not rescue the altered spleen size and the gross appearance of femur at 4 weeks posttransplantation. (H) The apparent difference of spleen and femur between WT and SHIP KO recipients and representative pictures of spleen and femur of a SHIP KO mouse at comparable age are also shown. (I) Quantification of the spleen weight difference. WBC, white blood cells (×10³); NE, neutrophils (×10³); LY, lymphocytes (×10³); RBC, red blood cells (×10⁶); PLT, platelets (×10⁵).
Data in (D), (E), (G) and (I) are mean ± SEM.*p < 0.05; **p < 0.01 (two-tailed t test). See also Figure S1.
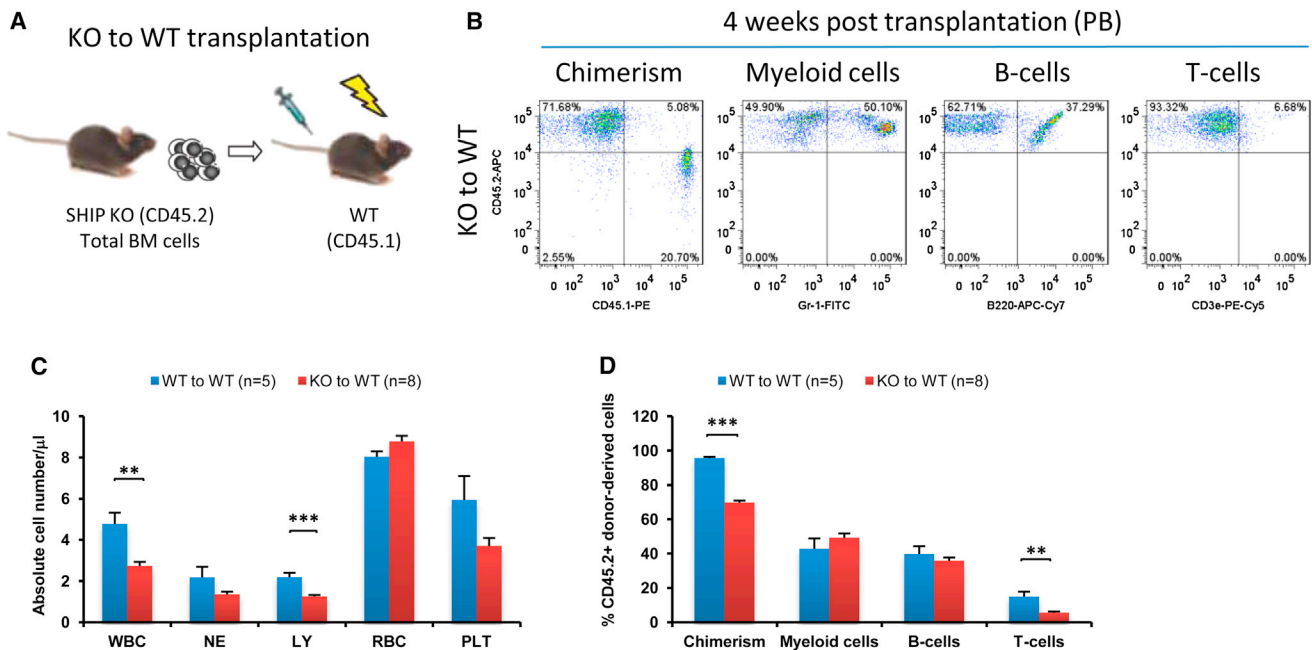
Figure 2. SHIP Disruption in Hematopoietic Lineages Led to Impaired Homing and Engraftment of These Cells but Was Not Responsible for the Hematopoiesis Defects Observed in the SHIP KO Mice
(A) Experimental design for transplant assays.
(B) Representative FACS lineage analysis.
(C) Absolute cell number in PB of WT transplant recipient mice. Total white blood cell count and lymphocyte count were lower in KO-to-WT transplant recipients.
(D) Donor-derived blood cell composition in PB of WT transplant recipient mice. Total donor chimerism and donor-derived T-cell percentage were lower in KO-to-WT transplant recipients. WBC, white blood cells ($\times 10^3$); NE, neutrophils ($\times 10^3$); LY, lymphocytes ($\times 10^3$); RBC, red blood cells ($\times 10^6$); PLT, platelets ($\times 10^5$). Data in (C) and (D) are mean ± SEM. **$p < 0.01$; ***$p < 0.001$ (two-tailed t test).

Interestingly, we also observed a reduced donor-derived T-cell production in the KO-to-WT recipient, indicating that SHIP may also play a role in T-cell recovery after irradiation.

SHIP Deficiency in the Niche Enables Its Reconstitution
Many genes, such as retinoic acid receptor γ (Walkley et al., 2007a), have been implicated in niche function. Disruption of these genes also leads to hematopoiesis defects. These defects remained even after the WT-to-KO reverse transplantation. Intriguingly, in the WT-to-SHIP KO recipients, the levels of both myeloid and B cell populations in PB shifted toward those of the WT-to-WT recipient mice at 8 and 12 weeks (Figure S1 available online) and 16 weeks after reverse transplantation (Figures 3A–3C; Figure S2G). The similar shift was also observed in the BM (Figures 3D and 3E; Figures S2A and S2B), although it was somewhat weaker compared to the shift in the PB (Figure 3E). The spleen size of the WT-to-KO recipients at 16 weeks was still larger than that of the WT-to-WT recipients, but it was significantly smaller compared to that of the KO-to-KO recipients (Figure 3F). Another prominent characteristic of the SHIP KO mouse is the elevated cellularity in the lung due to myeloid cell infiltration (Helgason et al., 1998). This phenotype was also significantly reversed to a much lesser extent in the WT-to-KO recipients (Figure 3G; Figure S2C). All of these results indicate that transplantation of WT whole BM cells may gradually reconstitute the BM microenvironment in SHIP-deficient mice.

We next directly investigated the structure of the BM. Hematoxylin and eosin (H&E) staining as well as immunohistochemical staining (IHC) using an antibody against adipocyte-specific perilipin of bone sections revealed that SHIP KO mice had no discernible adipocytes in the trabecular region of the femur and had significantly fewer adipocytes in the caudal vertebrae compared to WT mice (Figure 3H; Figures S2D and S2E). Subsequent histological analysis showed that the trabecular region of femurs of the WT-to-KO recipients contained numerous adipocytes similar to the WT-to-WT control mice, but in stark contrast to the KO-to-KO recipient mice (Figure 3I; Figure S2F). As illustrated in Figure 1H, pale femurs were phenotypical characteristics of SHIP KO mice (Figure 3I).

To definitively prove that transplantation of WT whole BM cells had reconstituted the BM microenvironment in the SHIP-deficient mice, a second reverse transplantation was performed in the CD45.1 chimera mice at 16 weeks after the first reverse transplantation (Figure 4A). Four weeks after the second reverse transplantation, similar to WT-to-WT recipients, WT-to-KO recipients exhibited a WT hematopoietic phenotype, in contrast to KO-to-KO recipients (Figures 4B–4D), confirming that SHIP KO chimera mice already possessed a WT BM microenvironment. To further demonstrate that a WT hematopoiesis had been established in the SHIP KO chimera mice, lineage⁻ (CD3e⁻, CD4⁻, CD8a⁻, B220⁻, CD19⁻, Gr-1⁻, and CD14⁻), Sca-1⁺, c-kit⁺ (LSK) hematopoietic stem and progenitor cells (Morrison and Weissman, 1994) were isolated from the
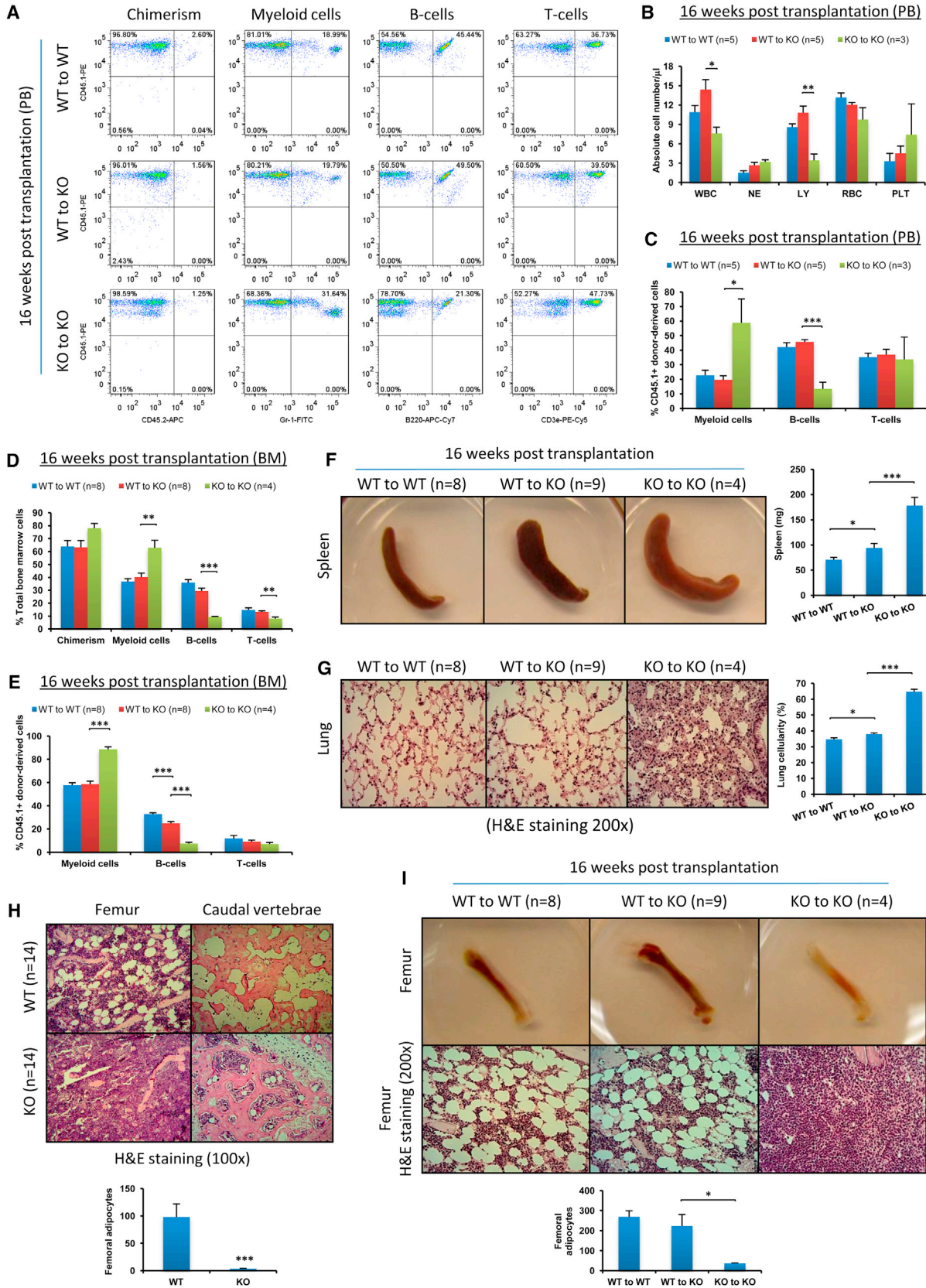
(legend on next page)

WT-to-KO recipients and transplanted into lethally irradiated WT mice (Figure 4E). As expected, all recipient mice exhibited a WT hematopoietic phenotype (Figures 4F–4H).

Nonhematopoietic Donor Cells Accomplish Niche Reconstitution

Transplantation of WT whole BM cells to SHIP KO mice converted the BM microenvironment from a SHIP KO phenotype to a WT phenotype. To determine which population of the transplanted WT BM cells contributed to the nonhematopoietic reconstitution in the SHIP KO recipient mice, we combined WT hematopoietic cells (CD45$^+$ and/or Ter119$^+$) (WT-HEM) and SHIP-deficient nonhematopoietic cells (CD45$^-$ and Ter119$^-$) (KO-N-HEM) in a ratio of 100:1, which is comparable to the composition found in normal BM (nonhematopoietic cells were approximately 0.5%–1% of the BM cells) and then transplanted them into lethally irradiated SHIP KO mice (Figure 5A). The resulting donor chimerism after transplantation was significantly lower than that of the WT (whole BM)-to-KO transplantation. Although the absolute numbers of donor-derived white blood cells were low at 4 weeks posttransplantation, they consisted primarily of myeloid cells with very few lymphocytes (Figures 5B–5D). This SHIP KO hematopoietic phenotype persisted at both 4 weeks and 16 weeks after transplantation (Figures 5E–5H), suggesting that WT hematopoietic donor cells were not sufficient to reconstitute the SHIP-deficient microenvironment and WT nonhematopoietic cells were critical for successful niche reconstitution. Consistently, the pathological phenotype associated with SHIP deficiency also remained when SHIP KO nonhematopoietic cells were used as donor cells (Figures 5I–5K). We also analyzed the number of LSK cells in the BM of WT-HEM + KO-N-HEM recipients, which appeared similar to that of SHIP KO mice (Figure 5L; Figure S3A). In a similar experiment, we transplanted WT hematopoietic cells alone (WT-HEM) into lethally irradiated SHIP KO mice (Figure 6A). Without WT nonhematopoietic cells, the resulting donor chimerism after transplantation was significantly lower than that of the WT (whole BM)-to-KO transplantation. Similarly, despite minuscule amount of donor-derived white blood cells, they consisted primarily of myeloid cells with very few lymphocytes, a phenotype of the SHIP KO mice (Figures 6B–6D). The recipient mice eventually died between 4 and 7 weeks posttransplantation (Figure 6E). We then adopted a technique reported by Morikawa et al. (2009) to isolate CD45$^-$, Ter119$^-$, PDGFRα$^+$, and Sca-1$^+$ (PαS) multipotent stromal cells from mouse BM (Figure 6F). We combined WT hematopoietic cells and WT PαS cells to transplant into lethally irradiated WT or SHIP KO mice (Figure 6G). After 16 weeks, SHIP KO recipients had significantly lower chimerism than WT recipients. However,

the SHIP KO recipients exhibited hematopoietic lineage composition in PB and BM comparable to that of the WT recipients (Figures 6H–6L). Collectively, these results demonstrate that WT hematopoietic cells alone were not sufficient to sustain hematopoiesis in lethally irradiated SHIP KO mice and WT nonhematopoietic cells, including the PαS cells, are required for the BM reconstitution in SHIP KO recipients.

We applied several different approaches to quantify nonhematopoietic chimerism in the BM of SHIP KO recipients. First, under rigorous gating conditions, we isolated CD45$^-$ and Ter119$^-$ nonhematopoietic cells from the BM (Figures 7A and 7B). We then used conventional PCR (Figure 7C) to detect and quantitative real-time PCR (Figure 7D) to measure WT SHIP DNA in SHIP KO recipients. Next, we quantified Y-chromosome-specific DNA in sex-mismatched recipients to demonstrate that while WT-to-KO transplantation resulted in chimerism, WT-to-WT transplantation did not (Figures 7E and 7F). Finally, we measured red fluorescent protein (RFP) DNA in donor-derived RFP-gene-positive cells in non-RFP recipients (Figures 7G and 7H). While there was no significant chimerism in WT-to-WT recipients, the nonhematopoietic chimerism estimated by all three quantitative PCR methods was about 30%–40% in the WT-to-KO recipients at 16 weeks after the reverse transplantation (Figures 7D, 7F, and 7H). In the above experiments, the targeted nonhematopoietic cell population is a mixture of multiple cell types, including multipotent BM stromal cells, fibroblasts (reticular connective tissue), and endothelial cells. In order to examine the reconstitution of multipotent stromal cells in the WT-to-KO recipients, we performed a colony-forming assay (CFU-Fs) (Friedenstein et al., 1974; Kuznetsov et al., 2009) with the CD45$^-$Ter119$^-$ BM cells from WT-to-KO recipients (Figure 7I). Total genomic DNA was isolated from individual colonies, and genotyping was performed to determine whether the cells were of WT donor or of SHIP KO recipient origin. The results indicated that up to 70% of the multipotent BM stromal cells of the KO recipients came from a WT donor (Figure 7J). Taken together, these results directly show that cells that originated from transplanted nonhematopoietic cells were indeed incorporated into the BM microenvironment in the SHIP KO recipient mice and suggest that there is a selective advantage to allow engraftment of WT nonhematopoietic cells in the SHIP KO BM microenvironment. It is noteworthy that in the third approach we used whole BM cells from RFP (or GFP) transgenic mice for transplantation. We initially intended to use fluorescence-activated cell sorting (FACS) to quantify nonhematopoietic chimerism in SHIP KO recipient mice. Interestingly, we discovered that BM cells in the nonhematopoietic compartment of the RFP or GFP mice were not fluorescent (Figure S4). It has been a problem in the BM stromal field that

Figure 3. Transplantation of WT Whole BM Cells Reversed the Hematopoietic Phenotype and Alleviated Pathology in the SHIP-Deficient Mice

(A–E) Transplantation of WT whole BM cells reversed the hematopoietic phenotype. (A) Representative FACS profiles of hematopoietic cell lineage analysis of PB from transplant recipients at 16 weeks posttransplantation. (B and C) Absolute blood cell number (B) and donor-derived blood cell composition (C) in PB of transplant recipients at 16 weeks posttransplantation. (D and E) Analysis of BM hematopoietic cell composition both in total BM cells (D) and in donor-derived cells (E). WBC, white blood cells (×10^3); NE, neutrophils (×10^3); LY, lymphocytes (×10^3); RBC, red blood cells (×10^6); PLT, platelets (×10^5).

(F–I) Transplantation of WT whole BM cells alleviated pathological phenotype and restored adipogenesis in the BM of SHIP-deficient mice. (F) Gross appearance of spleen and quantification of spleen weight of WT-to-WT, WT-to-KO, and KO-to-KO transplant recipients. (G) H&E staining of lung histological sections (200×) and quantification of lung cellularity of WT-to-WT, WT-to-KO, and KO-to-KO transplant recipients. (H) Representative femur and caudal vertebrae sections after H&E staining and quantification of femoral adipocytes in WT and SHIP KO mice. (I) Gross appearance of femur, H&E staining of femur sections, and quantification of femoral adipocytes of WT-to-WT, WT-to-KO, and KO-to-KO transplant recipients.

Data in (B), (C), (D), (E), (F), (G), (H), and (I) are mean ± SEM.*p < 0.05; **p < 0.01; ***p < 0.001 (two-tailed t test). See also Figure S2.
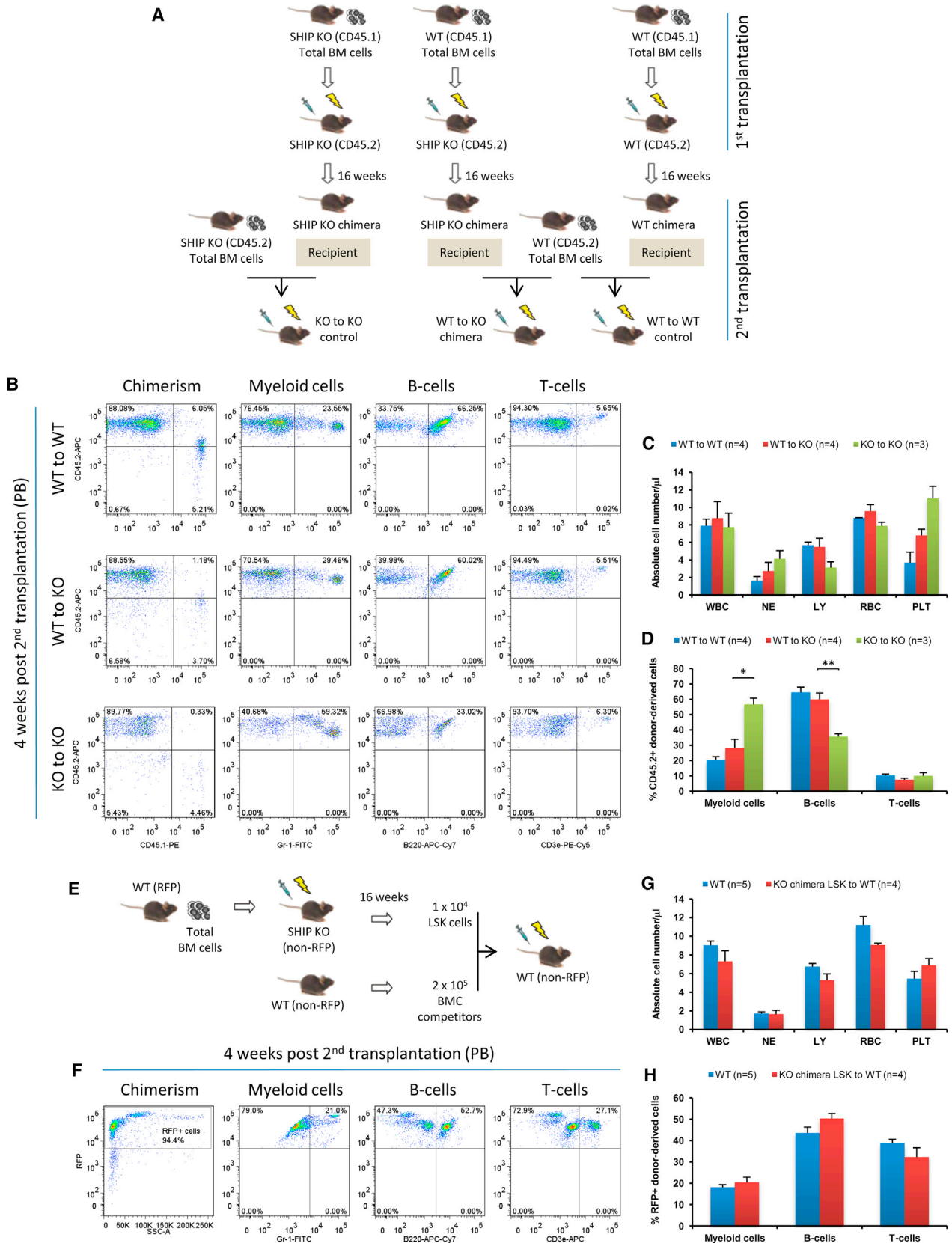
(legend on next page)

oftentimes a reporter gene is silenced in these cells for reasons that are not clear. In both mice, the expression of RFP or GFP is under the control of cytomegalovirus early enhancer/chicken β-actin (CAG) promoter. Despite the ability of the CAG promoter to drive gene expression in almost all tissues, its activity appears to be developmentally regulated in specific cell lineages (Baup et al., 2009). Accordingly, we decided to quantify the RFP DNA in the SHIP KO recipients using PCR instead (Figure 7H).

SHIP-Deficient BM Microenvironment

We next explored the mechanism by which the SHIP KO BM microenvironment affects normal hematopoiesis. Using a laser scanning cytometry imaging technique, we found that the SHIP KO mouse BM had a similar number and distribution of c-kit^{+} progenitor cells in the femur as WT mice despite the absence of adipocytes (Figures 8A–8C). Both WT and SHIP KO mouse BM contained comparable total number of cells. As previously reported, SHIP KO mouse BM contained 5-fold more LSK hematopoietic stem and progenitor cells (Figure 8D; Figure S3A). We also measured the amount of BM multipotent stromal cells, which can give rise to multiple mesenchymal cell lineages, including chondrocytes, osteocytes, and adipocytes. Intriguingly, SHIP KO mouse BM contained about 10-fold less CD45^{−}, CD11b^{−}, CD29^{+}, CD44^{+}, CD105^{+}, CD106^{+}, and Sca-1^{+} multipotent stromal cells (Zhu et al., 2010) (Figure 8E; Figure S3B) and about 1-fold less CD45^{−}, Ter119^{−}, PDGFRα^{+}, and Sca-1^{+} (PαS) multipotent stromal cells (Morikawa et al., 2009) (Figure 8F). Initial isolation of BM stromal cells based on their plastic-adherence properties (Peister et al., 2004) indicated that significantly more cells, presumably macrophages and monocytes, from the SHIP KO mouse BM adhered to the plastic tissue culture dish (Figure S5A). In a separate cell-adhesion assay under controlled shear flow, we could confirm that myeloid cells from SHIP KO mouse BM exhibited a higher degree of adhesion to a plastic surface than those from WT mouse BM (data not shown). We then performed a CFU-Fs (Friedenstein et al., 1974; Kuznetsov et al., 2009) using CD45^{−}Ter119^{−} BM stromal cells to exclude possible contamination from BM macrophages. The results indicated that both WT and SHIP KO BM stromal cells had similar abilities to form fibroblast-like colonies (Figure S5B).

In order to further study BM multipotent stromal cells, we isolated PαS multipotent stromal cells from WT and SHIP KO mouse BM (Figure 6F). SHIP KO PαS cells formed fewer adipocytes compared to WT PαS cells (Figure 8G). Interestingly, although SHIP KO PαS cells formed fewer adipocytes, these cells appeared to have produced more lipid droplets than WT

adipocytes as judged by oil red O staining (Figure 8G). Western blots of whole BM cells and IHC showed that SHIP KO BM adipocytes expressed a much higher level of adiponectin in both femur and caudal vertebrae compared to WT mice (Figure 8H; Figure S5C). Thus, the capability of fat-cell formation in vitro closely reflected the aforementioned in vivo observations of SHIP KO mouse BM. SHIP KO PαS cells also appeared to have an impaired ability to form an osteoblastic nodule upon osteogenic induction (Figures S5D and S5E). It is noteworthy that a previous study by Takeshita et al. showed that SHIP does not modulate bone formation in vivo (Takeshita et al., 2002; please also see Discussion).

It was recently reported that tumor suppressor retinoblastoma protein (RB) can regulate interactions between HSCs and BM microenvironment (Walkley et al., 2007b) as well as cell-fate choice and lineage commitment in vivo (Calo et al., 2010). However, the level of phospho-RB was similar between the WT and SHIP KO PαS cells (Figure 8I). Since progression of a cell through G1 and S phase requires inactivation of RB by phosphorylation (Harbour and Dean, 2000), similar level of phospho-RB indicates normal cell-cycle progression of SHIP KO PαS cells. Further investigation revealed that SHIP KO PαS cells expressed less FOXO1 and diminished levels of phospho-PPARγ but an equivalent level of total PPARγ compared with WT PαS cells (Figure 8I). Both FOXO1 and phosphorylation of PPARγ are known to inhibit PPARγ activities in adipogenesis (Hu et al., 1996; Nakae et al., 2003), and depletion of FOXO1 prevents osteoblast differentiation (Siqueira et al., 2011). SHIP KO PαS cells also expressed less AKT and phospho-AKT and produced a larger amount of the 12 kDa cleaved caspase-3 fragment (Figure 8I). Consistently, SHIP KO PαS cells were more prone to apoptosis in vitro under normal culture conditions when compared with WT PαS cells (Figure 8J). A recent study also showed that SHIP inhibition can cause apoptosis of hematopoietic cancer cells (Brooks et al., 2010). Starting with the same number of BM PαS cells, the total number of cells derived from SHIP KO PαS cells was about 40% less than that from the WT PαS cells in normal culture over 7 days (Figure 8K). We also observed that SHIP-deficient CD45^{−}Ter119^{−} BM stromal cells lost viability in long-term culture (Figures S5F and S5G). These results are consistent with earlier PαS cell isolation (Figure 8F) and apoptosis results (Figure 8J). While irradiated WT BM PαS cells recovered rapidly, the number of irradiated SHIP KO BM PαS cells did not increase over time (Figure 8L). Thus, the propensity of apoptosis and impaired growth after irradiation may contribute to the nonhematopoietic reconstitution by WT donor cells in the SHIP-deficient recipient mice.

Figure 4. Conversion to a Normal Hematopoietic Niche and Establishment of Normal Hematopoiesis in the SHIP KO Chimera

(A–D) Conversion to a normal hematopoietic niche in the SHIP KO chimera was confirmed by a second reverse transplantation. (A) BM cells of CD45.2 WT mice were transplanted into lethally irradiated WT CD45.1 chimeric mice or littermate SHIP KO CD45.1 chimeric mice. As a control, BM cells of CD45.2 SHIP KO mice were transplanted into lethally irradiated SHIP KO CD45.1 chimeric mice. (B) Representative FACS profiles of hematopoietic cell lineage analysis in PB of second reverse transplant recipients at 4 weeks posttransplantation. (C and D) The absolute blood cell number (C) and donor-derived blood cell composition (D) in PB of second reverse transplant recipients at 4 weeks posttransplantation.

(E–H) Normal hematopoiesis established in the SHIP KO chimera was confirmed by a secondary transplantation. (E) BM cells of red fluorescent protein (RFP) WT mice were transplanted into lethally irradiated SHIP KO mice. After 16 weeks, LSK hematopoietic stem and progenitor cells were isolated and transplanted into lethally irradiated WT mice. (F) Representative FACS profiles of hematopoietic cell lineage analysis in PB of secondary transplant recipients. (G and H) Absolute blood cell number (G) and donor-derived blood cell composition (H) in PB of secondary transplant recipients (red bars) compared with WT mice (blue bars). WBC, white blood cells (×10^{3}); NE, neutrophils (×10^{3}); LY, lymphocytes (×10^{3}); RBC, red blood cells (×10^{6}); PLT, platelets (×10^{5}). Data in (C), (D), (G), and (H) are mean ± SEM. *p < 0.05; **p < 0.01 (two-tailed t test).
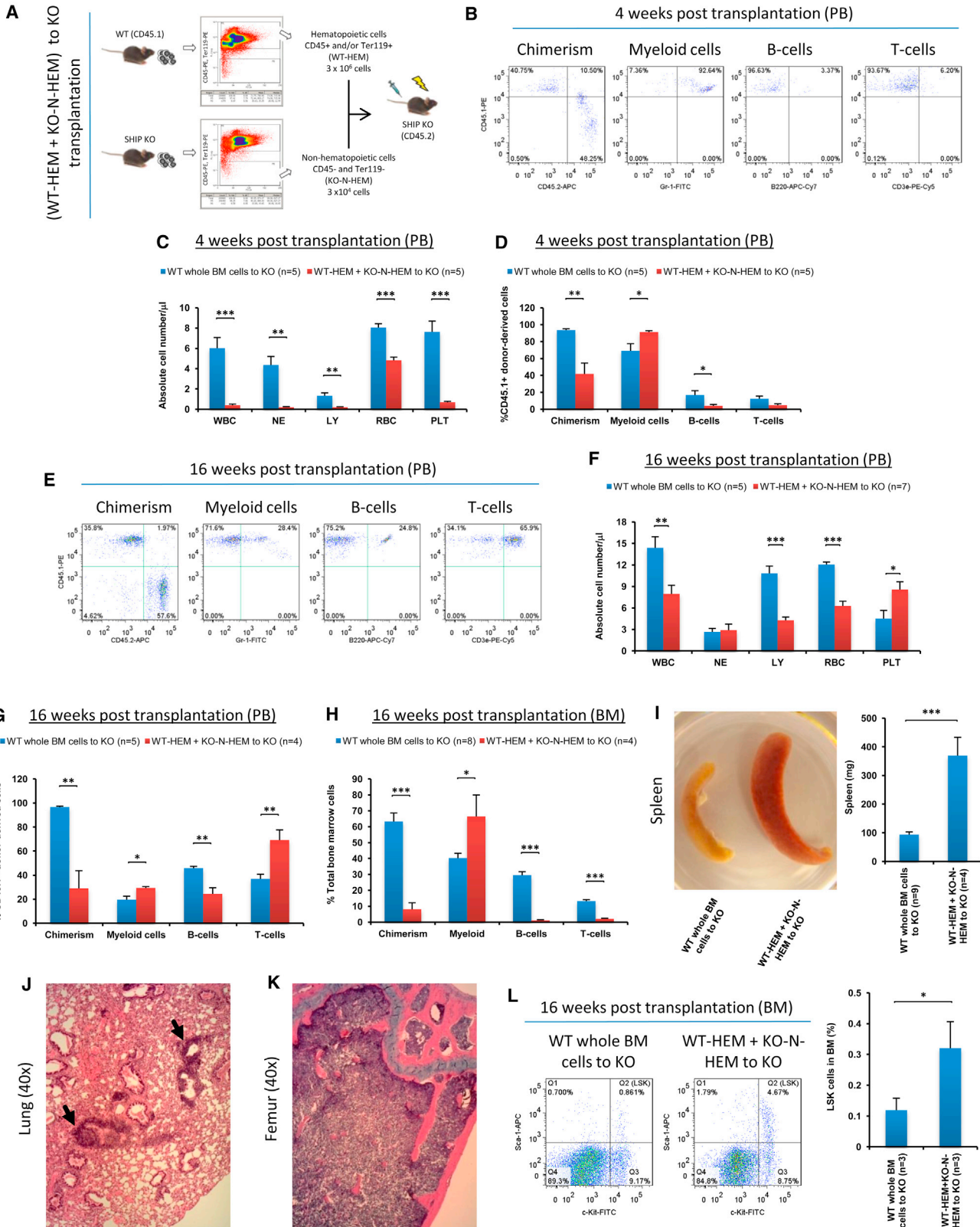
DISCUSSION

Hematopoiesis is the process by which all lineages of blood cells are produced in a hierarchical and stepwise manner in the BM, and at the apex of this hierarchy are the HSCs (Orkin and Zon, 2008). Previous studies suggested that SHIP might play a role in HSC signaling and thus HSC homeostasis, homing, and reconstituting potential (Desponts et al., 2006; Helgason et al., 2003). On further investigation, our data support the notion that SHIP KO mice have a distinct state of hematopoiesis that includes a defective hematopoietic cellular composition skewing toward myeloid cells at the cost of lymphopoiesis both in the PB and BM and have significantly more HSCs despite comparable total BM cellularity. A recent study by Hazen et al. suggested that the defective hematopoiesis in SHIP KO mice was not HSC cell autonomous (Hazen et al., 2009). In the present study, we provided direct evidence by using reverse transplantation to demonstrate that a SHIP-deficient BM microenvironment indeed can determine defective hematopoiesis at 4 weeks posttransplantation. However, this is the prelude of what we observed at later time points, when hematopoiesis in SHIP KO recipients was surprisingly normalized. We then investigated what might have caused such normalization, which revealed that a significant nonhematopoietic chimerism took place in the BM of SHIP KO mice. Thus, a significant nonhematopoietic chimerism resulting in a normal hematopoiesis has been demonstrated. Mechanistically, we studied PαS cells from the BM of SHIP KO mice and discovered that their distinct properties, including propensity of apoptosis and impaired growth after irradiation, may contribute to the nonhematopoietic chimerism. Furthermore, our results indicate that WT nonhematopoietic cells are required for the BM reconstitution in SHIP KO recipients.

Earlier studies by Hazen et al. also demonstrated that circulating levels of multiple cytokines were elevated in SHIP KO mice (Hazen et al., 2009). During the initial period following reverse transplantation of WT BM cells, aberrant cytokine levels were likely to persist in the BM microenvironment of SHIP KO recipients, which may have contributed to the SHIP KO hematopoietic phenotype observed at 4 weeks after transplantation. It is conceivable that once the WT nonhematopoietic cells have successfully engrafted and started to proliferate and differentiate, the reconstitution of the BM microenvironment in SHIP KO

mouse would take place, leading to normalization of hematopoiesis. On the other hand, it is also possible that the normal cytokine responsiveness of the WT hematopoietic progenitors contributed to the observed normalization of the hematopoiesis. To further dissect the potential mechanisms involved, we performed a series of experiments to validate our findings. First, whole BM cells from SHIP KO mice were transplanted into WT mice, and we found that overall levels of donor-derived myeloid cells and B cells were comparable between WT and SHIP KO cell recipients at 4 weeks after transplantation. At 16 weeks after the transplantation, the SHIP KO cell recipients exhibited elevated myelopoiesis and reduced lymphopoiesis as reported previously (Helgason et al., 2003). In the second set of experiments, hematopoietic cells from WT mice combined with nonhematopoietic cells from SHIP KO mice were transplanted into lethally irradiated SHIP KO mice. In this setting, however, the donor chimerism was so poor that total white blood cell levels in the SHIP KO recipients were extremely low. Interestingly, those successfully engrafted donor cells differentiated primarily into myeloid cells. In the third set of experiments, WT hematopoietic cells alone were transplanted into SHIP KO mice. They exhibited similar hematopoietic phenotype as WT-HEM + KO-N-HEM recipients. All the SHIP KO recipients in the latter experiment eventually died 4–6 weeks posttransplantation. In the next set of experiments, we combined WT hematopoietic cells and WT PαS cells to transplant into lethally irradiated SHIP KO mice, and these SHIP KO recipients exhibited a WT hematopoietic lineage composition in PB and BM after transplantation. Collectively, these experiments indicated that the nonhematopoietic reconstitution observed in the BM of SHIP KO mice was not caused by the transplanted WT hematopoietic cells and the WT nonhematopoietic cells, including the PαS cells, were required to establish normal hematopoiesis in the recipients.

Although there was no comprehensive study on hematopoiesis after a double irradiation and transplantation, tandem hematopoietic stem cell transplantation has been a feasible clinical option in treating patients with severe blood malignancies, where total body irradiation was only given in one transplant procedure (Monjanel et al., 2011; Somlo et al., 2011). Nevertheless, such tandem transplantation inspired us to perform a second reverse transplantation to demonstrate that SHIP KO chimeras, due to nonhematopoietic chimerism,

Figure 5. Transplanted WT Nonhematopoietic Cells Were Responsible for the Reconstitution of BM Microenvironment in the SHIP KO Recipients

(A) Strategy to combine WT hematopoietic cells (WT-HEM) and SHIP KO nonhematopoietic cells (KO-N-HEM) in the transplantation.

(B) Representative FACS profiles of donor-cell chimerism and hematopoietic cell lineage analysis of PB of WT-HEM + KO-N-HEM to KO transplant recipients at 4 weeks posttransplantation.

(C and D) Absolute blood cell number (C) and donor-derived blood cell composition (D) in PB of WT-HEM + KO-N-HEM to KO transplant recipients at 4 weeks posttransplantation.

(E–L) At 16 weeks posttransplantation, a SHIP KO hematopoietic phenotype and a pathological phenotype associated with SHIP deficiency persisted when WT nonhematopoietic donor cells were replaced with SHIP-deficient nonhematopoietic donor cells. (E) Representative FACS profiles of donor-cell chimerism and hematopoietic cell lineage analysis of PB of WT-HEM + KO-N-HEM to KO transplant recipients at 16 weeks posttransplantation. (F and G) Absolute blood cell number (F) and the percentage among donor-derived cell population (G) in the PB of transplant recipients at 16 weeks posttransplantation. (H) Total hematopoietic cell composition (percentage) in the BM of transplant recipients at 16 weeks posttransplantation. (I) Apparent and quantitative difference of spleen between WT whole BM recipients and WT-HEM + KO-N-HEM recipients at 16 weeks after reverse transplantation. (J) Elevated cellularity and myeloid infiltration (black arrows) remained visible in the lungs of WT-HEM + KO-N-HEM transplant recipients (n = 4). (K) No discernible adipocytes in the femurs of WT-HEM + KO-N-HEM transplant recipients (n = 4). (L) Representative FACS analysis (left) and quantification (right) of total BM LSK cells of WT whole BM recipients and WT-HEM + KO-N-HEM recipients at 16 weeks after reverse transplantation.

WBC, white blood cells ($\times 10^3$); NE, neutrophils ($\times 10^3$); LY, lymphocytes ($\times 10^3$); RBC, red blood cells ($\times 10^6$); PLT, platelets ($\times 10^5$). Data in (C), (D), (F), (G), (H), (I) and (L) are mean ± SEM.*p < 0.05; **p < 0.01; ***p < 0.001 (two-tailed t test). See also Figure S3.
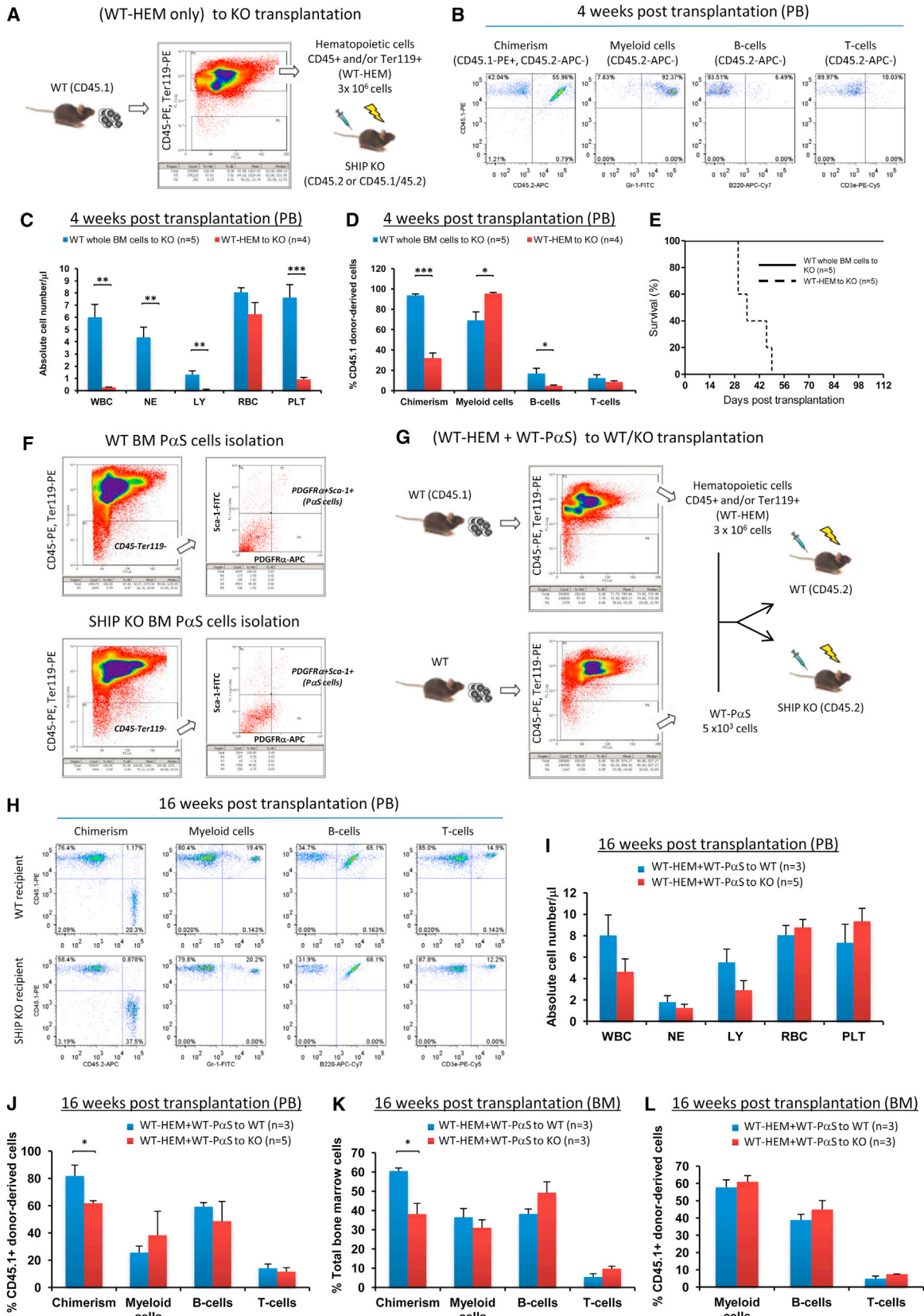
(legend on next page)

had a functional BM microenvironment capable of normal hematopoiesis. WT hematopoiesis established in the WT-to-KO transplant recipients was further confirmed by a secondary transplantation of the LSK hematopoietic stem and progenitor cells.

Despite the advance in understanding genetic events leading to pathogenesis of hematologic malignancies, significant improvements in therapeutic outcome based on these insights have not been forthcoming in many cases. A dysfunctional BM microenvironment is now also believed to contribute to disease development. Thus, one potential therapeutic strategy is to replace the defective microenvironment. So far, functional replacement of a diseased BM microenvironment through BM transplantation has not been possible. Despite the report by Rombouts and Ploemacher (2003), in most studies of murine experiments or in clinical transplantations where primary BM cells were infused, donor nonhematopoietic stromal cells could rarely be detected in the recipient BM (Laver et al., 1987; Morikawa et al., 2009; Simmons et al., 1987). Our results with WT recipients that had negligible nonhematopoietic chimerism in BM are consistent with these reports. Here, we show that lipid phosphatase SHIP deficiency may enable a functional reconstitution of BM microenvironment by WT cells. In this study, the total nonhematopoietic chimerism in SHIP KO BM at 16 weeks after transplantation was estimated to be about 30%–40%, which was capable of producing a WT hematopoietic phenotype both in PB and BM. To examine the reconstitution of multipotent stromal cells in the WT-to-KO recipients, we performed CFU-Fs with the CD45⁻Ter119⁻ BM cells from WT-to-KO recipients and found that up to 70% of the BM multipotent stromal cells of the KO recipients came from a WT donor. The numerous adipocytes seen in the WT-to-KO recipients strongly indicate that donor multipotent stromal cells were a major contributor in this reconstitution. The study by Morikawa et al. (2009) showed that primary PαS cells can home to appropriate sites and differentiate in response to cues from the niche environment. However, significant engraftment is only possible when the recipient's BM multipotent stromal cells were debilitated by standard conditioning in sufficient numbers to leave their niche available to the donor multipotent stromal cells. Indeed, the propensity of apoptosis of SHIP KO PαS cells and the lack of growth after irradiation could potentially facilitate their replacement by WT PαS cells. Although we showed that PαS cells were defective in the SHIP-deficient mice, this cell type is not exclusively functioning as a HSC niche. Normal hematopoiesis was restored only after the transplantation of WT PαS cells into the SHIP-deficient recipients. However, this finding cannot completely rule out the possibility that the

endogenous niche cells in the SHIP-deficient mice are also critical for hematopoiesis. The SHIP-deficient BM may still sustain different niche components such as osteoblastic cells and vascular cells. Additionally, considering the splenomegaly phenotype, it is possible that spleen may function as an alternative niche to rescue the defect in BM niche. Consistently, significant hematopoietic reconstitution was also observed in the niche-defective SHIP KO mice at 16 weeks posttransplantation (WT-HEM + KO-N-HEM to KO, Figures 5F–5H). Sacchetti et al. have identified perivascular cells as multipotent stem cells within the BM stroma (Sacchetti et al., 2007). Later, Mendez-Ferrer et al. reported a subset of perivascular multipotent stromal cells expressing nestin (Méndez-Ferrer et al., 2010), and Omatsu et al. provided new insight on the CXCL12-abundant reticular cells that support HSCs in BM (Omatsu et al., 2010). Besides osteogenic differentiation, these cells are also capable of differentiating into adipocytes, which are thought to exert an inhibitory role in hematopoiesis (Naveiras et al., 2009). Recently, Park et al. reported that BM-derived multipotent stromal cells may be a heterogeneous population with the newly identified Mx1⁺ population (Park et al., 2012). In addition, vascular cell adhesion molecule-1 was also reported to be a relevant marker for BM stromal cells (Chou et al., 2012). It is currently unclear whether or how much these cell populations overlap (Nombela-Arrieta et al., 2011).

The mechanisms triggering the reconstitution of hematopoietic inductive BM microenvironment in SHIP KO mice warrant future investigation. We speculate that the significantly lower multipotent stromal cell counts and their impaired function (e.g., defective adipogenesis and elevated apoptosis) in SHIP KO mice may contribute to the reconstitution. SHIP KO PαS cells are more prone to apoptosis and form fewer adipocytes in an in vitro adipogenesis assay compared to WT PαS cells. Consistently, our in vivo transplantation data also suggest defective adipogenesis of SHIP-deficient BM multipotent stromal cells. A small percentage of SHIP KO stromal cells can incorporate into the SHIP KO recipient mice (Figure 7F). However, these cells could never differentiate into mature adipocytes (Figure S2F). Hematopoiesis could also be regulated by osteoblastic niches. SHIP KO PαS cells appeared to have an impaired ability to form an osteoblastic nodule upon osteogenic induction in an in vitro assay (Figures S5D and S5E). However, a previous study by Takeshita et al. showed that SHIP does not modulate bone formation (osteogenesis) in vivo (Takeshita et al., 2002). Instead, due to an increased number of hyperresorptive osteoclasts, the three-dimensional trabecular volume fraction, trabecular thickness, number, and connectivity density of long bones are all

Figure 6. WT Nonhematopoietic BM Cells Were Required for the Reconstitution of BM Microenvironment in the SHIP KO Recipients
(A–E) WT hematopoietic cells alone were not sufficient to sustain hematopoiesis in lethally irradiated SHIP KO mice. (A) Strategy of experiments in which WT hematopoietic cells (CD45⁺ and/or Ter119⁺, WT-HEM) alone were transplanted into lethally irradiated SHIP KO mice. (B) Representative FACS analysis profile, (C) absolute blood cell number, and (D) donor-derived cell population in the PB of WT-HEM to KO recipients at 4 weeks posttransplantation. (E) Kaplan-Meier survival analysis of the recipients.
(F–L) WT PαS cells contribute to the formation of a hematopoietic microenvironment in the SHIP KO recipients. (F) Isolation of PαS cells by FACS sorting. Shown are representative FACS profiles of WT and SHIP KO PαS cells. (G) Strategy of experiments in which WT hematopoietic cells (CD45⁺ and/or Ter119⁺, WT-HEM) were combined with isolated WT-PαS cells to transplant into either WT or SHIP KO mice. (H) Representative FACS analysis profile. (I and J) Absolute blood cell number (I) and donor-derived cell population (J) in the PB at 16 weeks posttransplantation. (K and L) Analysis of BM hematopoietic cell composition both in total BM cells (K) and in donor-derived cells (L).
WBC, white blood cells (×10³); NE, neutrophils (×10³); LY, lymphocytes (×10³); RBC, red blood cells (×10⁶); PLT, platelets (×10⁵). Data in (C), (D), (I), (J), (K) and (L) are mean ± SEM.*p < 0.05; **p < 0.01; ***p < 0.001 (two-tailed t test).
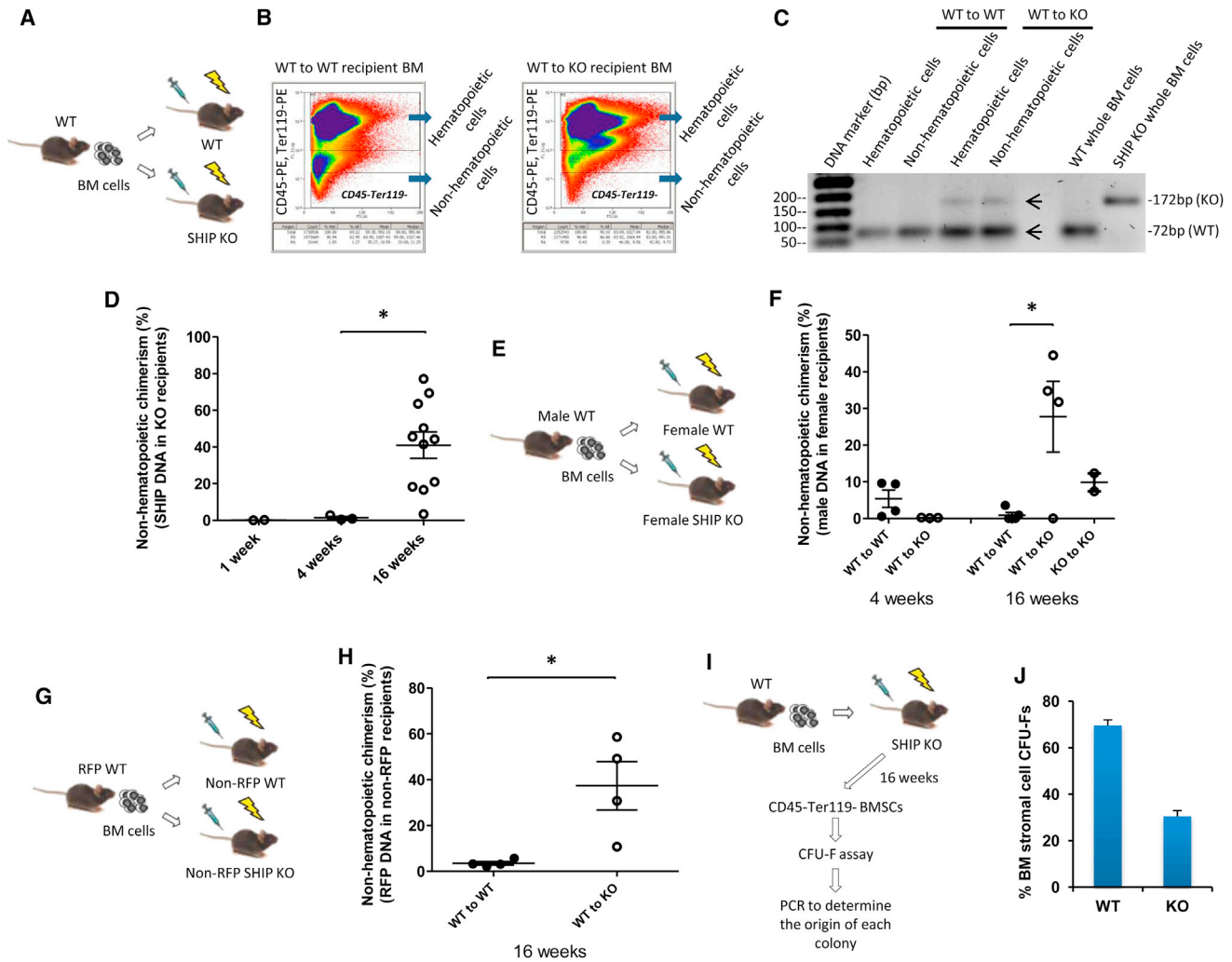
Figure 7. Quantification of Nonhematopoietic Chimerism in the SHIP KO Mouse BM Microenvironment

(A) Strategy to detect WT SHIP DNA in SHIP KO recipients.

(B) Representative FACS profile of isolation of hematopoietic cells (CD45^{+} and/or Ter119^{+}) and nonhematopoietic cells (CD45^{−} and Ter119^{−}) from WT and SHIP KO mouse recipient BM is shown.

(C) Conventional PCR genotyping of hematopoietic and nonhematopoietic cells from the BM of transplant recipients. The SHIP WT band (72 bp) and SHIP KO band (172 bp) are indicated.

(D) Quantitative real-time PCR determination of WT SHIP DNA in SHIP KO transplant recipients.

(E) Strategy to detect male DNA in female recipients.

(F) Quantitative real-time PCR determination of male DNA in female transplant recipients.

(G) Strategy to detect red fluorescent protein (RFP) reporter gene in non-RFP SHIP KO recipients.

(H) Quantitative real-time PCR determination of RFP reporter gene in non-RFP SHIP KO recipients. Nonhematopoietic cells from RFP BM were isolated by using APC-labeled anti-mouse CD45 and Ter119 antibodies.

(I) Strategy of colony-forming assay (CFU-Fs) with the CD45^{−}Ter119^{−} BM stromal cells from WT-to-KO recipients. Four SHIP KO recipients were used in this experiment; approximately 20 colonies from each mouse were selected for genomic DNA isolation.

(J) Conventional PCR was performed to determine the origin of individual colonies. Data are mean ± SEM.

*p < 0.05 (two-tailed t test). See also Figure S4.

slightly reduced in the SHIP KO mice (Takeshita et al., 2002). In current study, we carefully examined the bone structure. The thickness of the cortical bone was significantly reduced in the SHIP KO mice as previously reported (Takeshita et al., 2002). However, we could not detect significant increase or decrease in trabecular bone in the femur and caudal vertebra in the SHIP KO mice.

By using a specific nonhematopoietic cell type that is genetically labeled in the BM transplantation, the nonhematopoietic reconstitution in SHIP KO mice described here can be employed to visualize the donor cells' anatomic location after engraftment and to functionally assess hematopoietic outcome in the recipients when this specific cell type is excluded from the BM transplantation. Based on this model, the identity of the cells involved
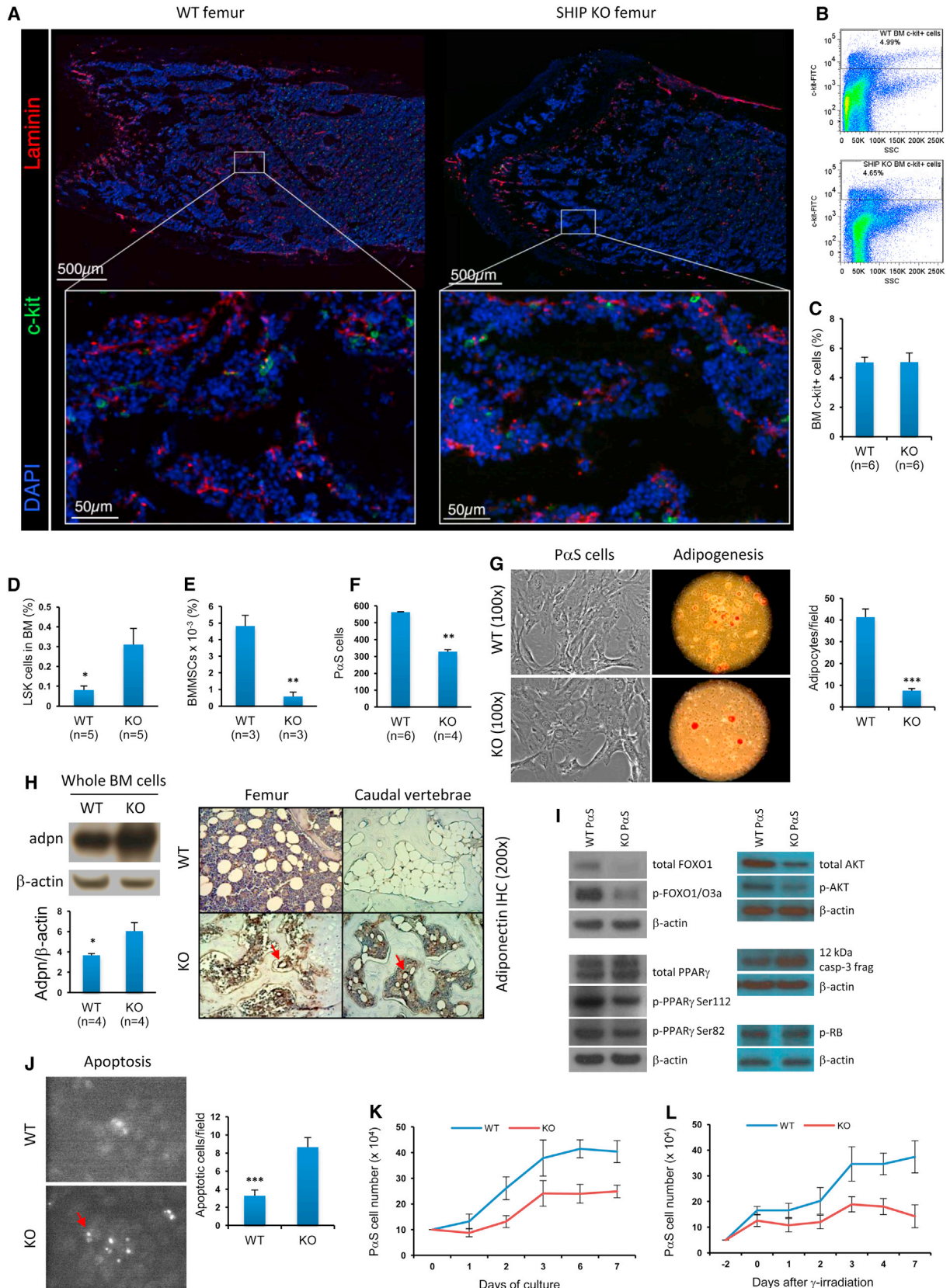
in a functional HSC microenvironment shall be investigated in the future. In a therapeutic setting, SHIP inhibition in patient's BM may be induced shortly before radiation therapy and transplantation of healthy donor BM cells. Hematopoiesis in the recipient patient may normalize once donor-derived nonhematopoietic cells have successfully engrafted and thrived. Taken together, our investigation suggests that nonhematopoietic reconstitution in SHIP KO mouse BM may provide a model to functionally study cell types involved in hematopoietic niches. More importantly, selective inhibition of SHIP in patients may improve treatment outcome by targeting both malignant hematopoietic cells and the aberrant BM microenvironment.

EXPERIMENTAL PROCEDURES

Mouse Maintenance and Genotyping

Animal procedures followed protocols approved by the Institutional Animal Care and Use Committee at Children's Hospital Boston. The SHIP KO mice were purchased from the Jackson Laboratory and maintained on a mixed genetic background (129/C57BL/6). SHIP heterozygous mice were backcrossed with either CD45.2$^+$ C57BL/6 mice or CD45.1$^+$ C57BL/6 mice (both from Jackson). Over a period of 2 years of backcrossing, we generated both CD45.2$^+$ SHIP KO mice in C57BL/6 background and CD45.1$^+$ SHIP KO mice in C57BL/6 background. Every donor and recipient mouse used in the transplantation experiments was carefully genotyped for its CD45.1 and/or CD45.2 expression before the actual experiment. For further details, see the Supplemental Experimental Procedures.

BM Cell Transplantation

Age-matched CD45.2$^+$ C57BL/6 and CD45.1 (B6.SJL-$Ptprc^a$/BoyAiTac) mice were purchased from Taconic (Hudson, NY). Donor whole BM cells were collected and transplantations were carried out following two rounds of 5.2 Gy lethal γ-irradiation of recipient mice performed 3 hours apart. For further details, see the Supplemental Experimental Procedures.

PαS Cell Isolation and Characterization

PαS cells were isolated and cultivated using reagents and methods as described by Morikawa et al. (2009). For further details, see Supplemental Experimental Procedures.

Determination of Nonhematopoietic Chimerism in the BM of SHIP KO Recipients

Conventional PCR genotyping was performed to detect the presence of WT and SHIP KO bands in hematopoietic and nonhematopoietic cells from the BM of SHIP KO recipients. Quantitative real-time PCR was performed using a CFX96 Thermal Cycler and iQ SYBR Green Supermix or iQ Multiplex Powermix from Bio-Rad. All primers were synthesized by Integrated DNA Technologies. For further details, see the Supplemental Experimental Procedures.

Statistics

Analysis of statistical significance for indicated data sets was performed using the Student's t test capability on Microsoft Excel and GraphPad Prism.

REFERENCES

Baup, D., Moser, M., Schurmans, S., and Leo, O. (2009). Developmental regulation of the composite CAG promoter activity in the murine T lymphocyte cell lineage. Genesis 47, 799–804.

Bianco, P. (2011). Bone and the hematopoietic niche: a tale of two stem cells. Blood 117, 5281–5288.

Bierkens, J.G., Hendry, J.H., and Testa, N.G. (1991). Recovery of the proliferative and functional integrity of mouse bone marrow in long-term cultures established after whole-body irradiation at different doses and dose rates. Exp. Hematol. 19, 81–86.

Brooks, R., Fuhler, G.M., Iyer, S., Smith, M.J., Park, M.Y., Paraiso, K.H., Engelman, R.W., and Kerr, W.G. (2010). SHIP1 inhibition increases immunoregulatory capacity and triggers apoptosis of hematopoietic cancer cells. J. Immunol. 184, 3582–3589.

Calo, E., Quintero-Estades, J.A., Danielian, P.S., Nedelcu, S., Berman, S.D., and Lees, J.A. (2010). Rb regulates fate choice and lineage commitment in vivo. Nature 466, 1110–1114.

Calvi, L.M., Adams, G.B., Weibrecht, K.W., Weber, J.M., Olson, D.P., Knight, M.C., Martin, R.P., Schipani, E., Divieti, P., Bringhurst, F.R., et al. (2003).

Figure 8. Characterization of SHIP-Deficient BM Microenvironment

(A–C) SHIP KO mouse BM had a similar number and distribution of c-kit$^+$ progenitor cells in the femur as WT mice. (A) Laser scanning cytometry imaging of the trabecular region of femur from WT and SHIP KO mice. Blood vessels (red) and c-kit$^+$ cells (green) were stained using specific antibodies against laminin and c-kit, respectively. Slides were counterstained with DAPI (blue). Images in the upper panel were composite of areas shown in the lower panel. Three mice were used in each group. (B and C) Analysis of c-kit$^+$ cell population showing similar numbers in WT and SHIP KO mouse BM.

(D–L) Disruption of SHIP led to reduced BM multipotent stromal cell (BMMSC) population, impaired adipogenic differentiation, and enhanced apoptosis of these cells. Comparison of LSK (D) and BMMSC (CD45$^-$, CD11b$^-$, CD29$^+$, CD44$^+$, CD105$^+$, CD106$^+$, and Sca-1$^+$) (E) populations between WT and SHIP KO mouse BM. (F) Comparison of PαS cell (CD45$^-$, Ter119$^-$, PDGFRα$^+$, and Sca-1$^+$) populations between WT and SHIP KO mouse BM. Shown are average PαS cell numbers obtained from two pairs of femur and tibia. (G) SHIP KO PαS cells formed fewer adipocytes compared to WT PαS cells. The adipogenic potential was assessed by oil red O staining (100×) at 14 days after adipogenic induction of WT and SHIP KO PαS cells. (H) SHIP KO adipocytes expressed much higher level of adiponectin in both femur and caudal vertebrae compared to WT mice. Western blots of whole BM cells (left) and IHC staining (right) were conducted using specific antibodies against adiponectin. Red arrows in IHC indicate adipocytes in SHIP KO mouse BM. (I) Western blots of key regulators of adipogenic process, cell-cycle progression, and markers of apoptotic process. (J) SHIP KO PαS cells were more prone to apoptosis in vitro. Apoptosis was assessed by TUNEL staining (100×). (K) Representative growth curves of WT and SHIP KO PαS cells in regular culture. (L) Representative growth curves of WT and SHIP KO PαS cells after γ-irradiation. Data in (C), (D), (E), (F), (G), (H), (J), (K), and (L) are mean ± SEM. *p < 0.05; **p < 0.01; ***p < 0.001 (two-tailed t test). See also Figure S5.

Osteoblastic cells regulate the haematopoietic stem cell niche. Nature *425*, 841–846.

Chou, D.B., Sworder, B., Bouladoux, N., Roy, C.N., Uchida, A.M., Grigg, M., Robey, P.G., and Belkaid, Y. (2012). Stromal-derived IL-6 alters the balance of myeloerythroid progenitors during Toxoplasma gondii infection. J. Leukoc. Biol. *92*, 123–131.

Colmone, A., Amorim, M., Pontier, A.L., Wang, S., Jablonski, E., and Sipkins, D.A. (2008). Leukemic cells create bone marrow niches that disrupt the behavior of normal hematopoietic progenitor cells. Science *322*, 1861–1865.

Desponts, C., Hazen, A.L., Paraiso, K.H., and Kerr, W.G. (2006). SHIP deficiency enhances HSC proliferation and survival but compromises homing and repopulation. Blood *107*, 4338–4345.

Ding, L., Saunders, T.L., Enikolopov, G., and Morrison, S.J. (2012). Endothelial and perivascular cells maintain haematopoietic stem cells. Nature *481*, 457–462.

Flynn, C.M., and Kaufman, D.S. (2007). Donor cell leukemia: insight into cancer stem cells and the stem cell niche. Blood *109*, 2688–2692.

Friedenstein, A.J., Deriglasova, U.F., Kulagina, N.N., Panasuk, A.F., Rudakowa, S.F., Luriá, E.A., and Ruadkow, I.A. (1974). Precursors for fibroblasts in different populations of hematopoietic cells as detected by the in vitro colony assay method. Exp. Hematol. *2*, 83–92.

Harbour, J.W., and Dean, D.C. (2000). Rb function in cell-cycle regulation and apoptosis. Nat. Cell Biol. *2*, E65–E67.

Hazen, A.L., Smith, M.J., Desponts, C., Winter, O., Moser, K., and Kerr, W.G. (2009). SHIP is required for a functional hematopoietic stem cell niche. Blood *113*, 2924–2933.

Helgason, C.D., Antonchuk, J., Bodner, C., and Humphries, R.K. (2003). Homeostasis and regeneration of the hematopoietic stem cell pool are altered in SHIP-deficient mice. Blood *102*, 3541–3547.

Helgason, C.D., Damen, J.E., Rosten, P., Grewal, R., Sorensen, P., Chappel, S.M., Borowski, A., Jirik, F., Krystal, G., and Humphries, R.K. (1998). Targeted disruption of SHIP leads to hemopoietic perturbations, lung pathology, and a shortened life span. Genes Dev. *12*, 1610–1620.

Hu, E., Kim, J.B., Sarraf, P., and Spiegelman, B.M. (1996). Inhibition of adipogenesis through MAP kinase-mediated phosphorylation of PPARgamma. Science *274*, 2100–2103.

Jones, D.L., and Wagers, A.J. (2008). No place like home: anatomy and function of the stem cell niche. Nat. Rev. Mol. Cell Biol. *9*, 11–21.

Kiel, M.J., Yilmaz, O.H., Iwashita, T., Yilmaz, O.H., Terhorst, C., and Morrison, S.J. (2005). SLAM family receptors distinguish hematopoietic stem and progenitor cells and reveal endothelial niches for stem cells. Cell *121*, 1109–1121.

Kuznetsov, S.A., Mankani, M.H., Bianco, P., and Robey, P.G. (2009). Enumeration of the colony-forming units-fibroblast from mouse and human bone marrow in normal and pathological conditions. Stem Cell Res. (Amst.) *2*, 83–94.

Lane, S.W., Scadden, D.T., and Gilliland, D.G. (2009). The leukemic stem cell niche: current concepts and therapeutic opportunities. Blood *114*, 1150–1157.

Laver, J., Jhanwar, S.C., O'Reilly, R.J., and Castro-Malaspina, H. (1987). Host origin of the human hematopoietic microenvironment following allogeneic bone marrow transplantation. Blood *70*, 1966–1968.

Li, L., and Neaves, W.B. (2006). Normal stem cells and cancer stem cells: the niche matters. Cancer Res. *66*, 4553–4557.

Li, X.M., Hu, Z., Jorgenson, M.L., Wingard, J.R., and Slayton, W.B. (2008). Bone marrow sinusoidal endothelial cells undergo nonapoptotic cell death and are replaced by proliferating sinusoidal cells in situ to maintain the vascular niche following lethal irradiation. Exp. Hematol. *36*, 1143–1156.

Liu, Q., Sasaki, T., Kozieradzki, I., Wakeham, A., Itie, A., Dumont, D.J., and Penninger, J.M. (1999). SHIP is a negative regulator of growth factor receptor-mediated PKB/Akt activation and myeloid cell survival. Genes Dev. *13*, 786–791.

Lo Celso, C., Fleming, H.E., Wu, J.W., Zhao, C.X., Miake-Lye, S., Fujisaki, J., Côté, D., Rowe, D.W., Lin, C.P., and Scadden, D.T. (2009). Live-animal tracking of individual haematopoietic stem/progenitor cells in their niche. Nature *457*, 92–96.

Méndez-Ferrer, S., Michurina, T.V., Ferraro, F., Mazloom, A.R., Macarthur, B.D., Lira, S.A., Scadden, D.T., Ma'ayan, A., Enikolopov, G.N., and Frenette, P.S. (2010). Mesenchymal and haematopoietic stem cells form a unique bone marrow niche. Nature *466*, 829–834.

Monjanel, H., Deconinck, E., Perrodeau, E., Gastinne, T., Delwail, V., Moreau, A., François, S., Berthou, C., Gyan, E., and Milpied, N.; GOELAMS. (2011). Long-term follow-up of tandem high-dose therapy with autologous stem cell support for adults with high-risk age-adjusted international prognostic index aggressive non-Hodgkin Lymphomas: a GOELAMS pilot study. Biol. Blood Marrow Transplant. *17*, 935–940.

Morikawa, S., Mabuchi, Y., Kubota, Y., Nagai, Y., Niibe, K., Hiratsu, E., Suzuki, S., Miyauchi-Hara, C., Nagoshi, N., Sunabori, T., et al. (2009). Prospective identification, isolation, and systemic transplantation of multipotent mesenchymal stem cells in murine bone marrow. J. Exp. Med. *206*, 2483–2496.

Morrison, S.J., and Weissman, I.L. (1994). The long-term repopulating subset of hematopoietic stem cells is deterministic and isolatable by phenotype. Immunity *1*, 661–673.

Morrison, S.J., and Spradling, A.C. (2008). Stem cells and niches: mechanisms that promote stem cell maintenance throughout life. Cell *132*, 598–611.

Nakae, J., Kitamura, T., Kitamura, Y., Biggs, W.H., 3rd, Arden, K.C., and Accili, D. (2003). The forkhead transcription factor Foxo1 regulates adipocyte differentiation. Dev. Cell *4*, 119–129.

Naveiras, O., Nardi, V., Wenzel, P.L., Hauschka, P.V., Fahey, F., and Daley, G.Q. (2009). Bone-marrow adipocytes as negative regulators of the haematopoietic microenvironment. Nature *460*, 259–263.

Nombela-Arrieta, C., Ritz, J., and Silberstein, L.E. (2011). The elusive nature and function of mesenchymal stem cells. Nat. Rev. Mol. Cell Biol. *12*, 126–131.

Omatsu, Y., Sugiyama, T., Kohara, H., Kondoh, G., Fujii, N., Kohno, K., and Nagasawa, T. (2010). The essential functions of adipo-osteogenic progenitors as the hematopoietic stem and progenitor cell niche. Immunity *33*, 387–399.

Orkin, S.H., and Zon, L.I. (2008). Hematopoiesis: an evolving paradigm for stem cell biology. Cell *132*, 631–644.

Park, D., Spencer, J.A., Koh, B.I., Kobayashi, T., Fujisaki, J., Clemens, T.L., Lin, C.P., Kronenberg, H.M., and Scadden, D.T. (2012). Endogenous bone marrow MSCs are dynamic, fate-restricted participants in bone maintenance and regeneration. Cell Stem Cell *10*, 259–272.

Peister, A., Mellad, J.A., Larson, B.L., Hall, B.M., Gibson, L.F., and Prockop, D.J. (2004). Adult stem cells from bone marrow (MSCs) isolated from different strains of inbred mice vary in surface epitopes, rates of proliferation, and differentiation potential. Blood *103*, 1662–1668.

Purton, L.E., and Scadden, D.T. (2008). The hematopoietic stem cell niche. In StemBook, ed. The Stem Cell Research Community, StemBook, http://dx.doi.org/10.3824/stembook.1.28.1, http://www.stembook.org.

Raab, M.S., Podar, K., Breitkreutz, I., Richardson, P.G., and Anderson, K.C. (2009). Multiple myeloma. Lancet *374*, 324–339.

Raaijmakers, M.H., Mukherjee, S., Guo, S., Zhang, S., Kobayashi, T., Schoonmaker, J.A., Ebert, B.L., Al-Shahrour, F., Hasserjian, R.P., Scadden, E.O., et al. (2010). Bone progenitor dysfunction induces myelodysplasia and secondary leukaemia. Nature *464*, 852–857.

Rohrschneider, L.R., Fuller, J.F., Wolf, I., Liu, Y., and Lucas, D.M. (2000). Structure, function, and biology of SHIP proteins. Genes Dev. *14*, 505–520.

Rombouts, W.J., and Ploemacher, R.E. (2003). Primary murine MSC show highly efficient homing to the bone marrow but lose homing ability following culture. Leukemia *17*, 160–170.

Sacchetti, B., Funari, A., Michienzi, S., Di Cesare, S., Piersanti, S., Saggio, I., Tagliafico, E., Ferrari, S., Robey, P.G., Riminucci, M., and Bianco, P. (2007). Self-renewing osteoprogenitors in bone marrow sinusoids can organize a hematopoietic microenvironment. Cell *131*, 324–336.

Schofield, R. (1978). The relationship between the spleen colony-forming cell and the haemopoietic stem cell. Blood Cells *4*, 7–25.

Simmons, P.J., Przepiorka, D., Thomas, E.D., and Torok-Storb, B. (1987). Host origin of marrow stromal cells following allogeneic bone marrow transplantation. Nature *328*, 429–432.

Siqueira, M.F., Flowers, S., Bhattacharya, R., Faibish, D., Behl, Y., Kotton, D.N., Gerstenfeld, L., Moran, E., and Graves, D.T. (2011). FOXO1 modulates osteoblast differentiation. Bone *48*, 1043–1051.

Somlo, G., Spielberger, R., Frankel, P., Karanes, C., Krishnan, A., Parker, P., Popplewell, L., Sahebi, F., Kogut, N., Snyder, D., et al. (2011). Total marrow irradiation: a new ablative regimen as part of tandem autologous stem cell transplantation for patients with multiple myeloma. Clin. Cancer Res. *17*, 174–182.

Spangrude, G.J., Heimfeld, S., and Weissman, I.L. (1988). Purification and characterization of mouse hematopoietic stem cells. Science *241*, 58–62.

Sugiyama, T., Kohara, H., Noda, M., and Nagasawa, T. (2006). Maintenance of the hematopoietic stem cell pool by CXCL12-CXCR4 chemokine signaling in bone marrow stromal cell niches. Immunity *25*, 977–988.

Taichman, R.S. (2005). Blood and bone: two tissues whose fates are intertwined to create the hematopoietic stem-cell niche. Blood *105*, 2631–2639.

Takeshita, S., Namba, N., Zhao, J.J., Jiang, Y., Genant, H.K., Silva, M.J., Brodt, M.D., Helgason, C.D., Kalesnikoff, J., Rauh, M.J., et al. (2002). SHIP-deficient mice are severely osteoporotic due to increased numbers of hyper-resorptive osteoclasts. Nat. Med. *8*, 943–949.

Till, J.E., and McCulloch, E.A. (1961). A direct measurement of the radiation sensitivity of normal mouse bone marrow cells. Radiat. Res. *14*, 213–222.

Walkley, C.R., Olsen, G.H., Dworkin, S., Fabb, S.A., Swann, J., McArthur, G.A., Westmoreland, S.V., Chambon, P., Scadden, D.T., and Purton, L.E. (2007a). A microenvironment-induced myeloproliferative syndrome caused by retinoic acid receptor gamma deficiency. Cell *129*, 1097–1110.

Walkley, C.R., Shea, J.M., Sims, N.A., Purton, L.E., and Orkin, S.H. (2007b). Rb regulates interactions between hematopoietic stem cells and their bone marrow microenvironment. Cell *129*, 1081–1095.

Xie, Y., Yin, T., Wiegraebe, W., He, X.C., Miller, D., Stark, D., Perko, K., Alexander, R., Schwartz, J., Grindley, J.C., et al. (2009). Detection of functional haematopoietic stem cell niche using real-time imaging. Nature *457*, 97–101.

Zhang, J., Niu, C., Ye, L., Huang, H., He, X., Tong, W.G., Ross, J., Haug, J., Johnson, T., Feng, J.Q., et al. (2003). Identification of the haematopoietic stem cell niche and control of the niche size. Nature *425*, 836–841.

Zhu, H., Guo, Z.K., Jiang, X.X., Li, H., Wang, X.Y., Yao, H.Y., Zhang, Y., and Mao, N. (2010). A protocol for isolation and culture of mesenchymal stem cells from mouse compact bone. Nat. Protoc. *5*, 550–560.